Analysis of Thermal radiation effects on MHD flow of a nanofluid over an exponentially stretching sheet with heat and mass fluxes in the occurrence of viscous dissipation

PARAKAPALI ROJA[1], THUMMALA SANKAR REDDY[1], SHAIK MOHAMMED IBRAHIM[3], GIULIO LORENZINI[4*]

[1]Department of Mathematics, Annamacharya Institute of Technology and sciences, Rajmpeta, Kadapa Andhra Pradesh-516126, INDIA

[2]Department of Mathematics, Annamacharya Institute of Technology and sciences, C. K. Dinne, Kadapa Andhra Pradesh-516003, INDIA

[3]Department of Mathematics, Koneru Lakshmaiah Education Foundation, Vaddeswaram, Guntur, Andhra Pradesh- 522302, INDIA

[4]Department of Engineering and Architecture, University of Parma, Parco Area delleScienze 181/A, Parma 43124, ITALY

Abstract: The numerical analysis of thermal emission on a magneto-hydrodynamics (MHD) stream of a viscous in-compressible nano-fluid due to an exponentially stretched sheet with warm and mass fluxes frontier conditions in the occurrence of viscous dissipation were examined in this work. Using self-similarity transformation, the controlling PDEs are altered into a set of ODEs, which are after that numerically solved via the shooting procedure and a 4^{th} Runge-Kutta method. On the non-dimensional stream, temperature, nano-particle capacity percent, and confined Nusselt and Sherwood figures, the consequences of many miscellaneous constraints are illustrated. The mathematical values of the friction factor coefficient, as well as confined Nusselt and Sherwood statistics, are computed and examined.

Keywords: *Thermal Emission; MHD; Nanofluid; heat and mass fluxes; Viscous Dissipation.*
Received: August 8, 2021. Revised: April 12, 2022. Accepted: May 15, 2022. Published: June 14, 2022.

1. Introduction

Because of its wide range of applications, such like continuous casting, exchangers, metal spinning, bundle wrapping, foodstuff processing, substance processing, equipment, in addition to polymer extrusion, the analysis of velocity and heat transport over a stretched surface has gotten a lot of awareness in modern years. The Newtonian runny stream induced by a stretched sheet was initially

studied by Crane [1]. Many researchers, including Dutta et al. [2], Chen and Char [3], and Gupta [4], improved Crane's [1] work by considering the influence of mass transport in diverse situations. The exponential stretched sheet was used by Nadeem et al. [5] to explore the heat transmission phenomenon of a water-based nanofluid. Bhattacharyya [6] investigated frontier layer stream and heat conduction across a sheet that was shrinking rapidly.

The high temperature transport stream through a permeable exponential stretched sheet with thermal emission was studied by Mukhopadhyay et al. [7]. The influence of heat emission on the frontier layer stream owing to an exponentially stretched sheet was studied by Sajid and Hayat [8]. Zhang et al. [9] focuses on the heat transport of a power law nanofluid thin film caused by a stretched sheet in the occurrence of stream slip and magnetic field. Majeed et al. [10] demonstrate ferromagnetic fluid frontier layer stream across a stretched surface. Pal and Saha [11] investigated the warm and mass transmission in a thin liquid film with the influence of non linear thermal emission using an unstable stretched sheet. Weidman [12] investigated a unified formulation for stagnation point streams including stretched surfaces.

MHD stream of an electrically conducting runny over a stretched sheet has out of the ordinary uses in modern metallurgical and metal-working techniques. Many professional polymer processes include pulling continuous strips and filaments from a moving fluid to cool them. The pace of cooling, which is determined by the structure of the frontierlayer adjacent to the stretched sheet, has a significant impact on the final result. MHD stream of Casson fluid due to exponentially stretched sheet with heat emission was explored by Mukhopadhyay et al. [13]. Hayat et al. [14] describe the consequence of magnetahydrodynamics on bidirectional nanofluid stream with second order slip stream and homogeneous–heterogeneous reactions.

Lin et al. [15] investigated the stream and heat transport of an unsteady MHD pseudo-plastic nanofluid in a finite thin film over a stretched surface with internal heat generation. Sheikholeslami et al. [16] used a two-phase model to investigate the consequence of thermal emission on magnetohydrodynamics nanofluid stream and heat transmission. Farooq et al. [17] demonstrate the use of the HAM-based Mathematica tool BVP h 2.0 on MHD Falkner–Skan nanofluid stream. Shehzad et al. [18] conducted an analytical study to examine thermal emission consequences in three-dimensional Jeffrey nanofluid stream with internal heat generation and magnetic field.

In procedures carried out at extremely high temperatures, the importance of emission cannot be overstated. Gas turbines, missiles, aircraft, space vehicles, and nuclear power plants all use radiative consequences. Moradi et al. [19] investigate the interplay of emission in a thermally convective viscous liquid stream over an inclined surface. Sheikholeslami et al. [20] used the two phasemodel to study the influence of emission in viscous nanofluid stream. Hayat et al. [21] investigate the laminar stream of an Oldroyd-B liquid with nanoparticles and emission. The radiative three-dimensional stream of Maxwell fluid with thermophoresis and convective condition was researched by Ashraf et al. [22]. Hayat et al. [23] investigated the heat emission in a Powell-Eyring nanofluid laminar stream over a stretched sheet.

Bidin and Nazar [24] investigated the influence of thermal emission on the constant laminar two-dimensional frontierlayer stream and heat transport over an exponentially stretched sheet. Using the Runge–Kutta fourth-order approach, Hady et al. [25] investigated the emission influence on viscous nanofluid over nonlinear stretched sheet. Hayat et al. [26] investigated the consequences of Joule heating and thermophoresis in a Maxwell model stretched stream under convection. Mustafa et al. [27] address Sakiadis stream of Maxwell fluid with convective frontiercondition. Hayat et al. [28] investigated the Maxwell fluid's stagnation point stream in the occurrence of thermal emission and convection. Hayat et al. [29] investigated the consequences of an angled field of magnetic and generating of heat in nanofluid stream with non-linear thermal emission. Khan et al. [30] investigate the nonlinear radiative stream of a three-dimensional Burgers nanofluid with a new mass flux consequence.

The goal of this explore is to probe the consequence of thermal emission on the magnetahydrodynamic (MHD) stream of a viscous incompressible nano sized particle fluid appropriate to an exponentially stretched sheet with warm and

massfluxes conditions in the occurrence of viscous dissipation numerically. The controlling PDEs are distorted into self-similar ODEs passing through similarity transformations, and subsequently solved numerically via the shooting practice.

2. Mathematical Formulation

An exponentially extending sheet is used to model the two-dimensional hydromagnetic stream of an incompressible fluid. The occurrence of thermal emission, viscous dissipation, a generating of heat, and a chemical reaction characterises warm and mass transport analysis. In the y-direction, a non-uniform magnetic field B(x) = B0exp(x/2l) is applied. For lower magnetic Reynolds statistics, the induced magnetic field is ignored. At the sheet's surface, we imposed warm and mass flux frontier conditions. The subsequent are the principal equations of movement:

(i) Continuity:

$$\frac{\partial u}{\partial x}+\frac{\partial u}{\partial y}=0 \tag{1}$$

(ii) Momentum:

$$u\frac{\partial u}{\partial x}+v\frac{\partial u}{\partial y}=\nu\frac{\partial^2 u}{\partial y^2}-\frac{\sigma B_0^2}{\rho}u \tag{2}$$

(iii) Energy:

$$u\frac{\partial T}{\partial x}+v\frac{\partial T}{\partial y}=\alpha\frac{\partial^2 T}{\partial y^2}+\frac{(\rho c)_p}{(\rho c)_f}\left[D_B\frac{\partial C}{\partial y}\frac{\partial T}{\partial y}+\frac{D_T}{T_\infty}\left(\frac{\partial T}{\partial y}\right)^2\right] -\frac{1}{\rho c_p}\frac{\partial q_r}{\partial y}+\frac{\mu}{\rho c_p}\left(\frac{\partial u}{\partial y}\right)^2 \tag{3}$$

(iv) Nanoparticle volume fraction:

$$u\frac{\partial N}{\partial x}+v\frac{\partial N}{\partial y}=D_B\frac{\partial^2 N}{\partial y^2}+\frac{D_T}{T_\infty}\frac{\partial^2 T}{\partial y^2} \tag{4}$$

subject to the frontier conditions:

$$u=U_w(x)=\mathrm{U}_0\exp\left(\frac{x}{l}\right),\ v=-V(x),$$
$$\frac{\partial T}{\partial y}=-\frac{q_w(x)}{\alpha},\ \frac{\partial N}{\partial y}=-\frac{q_{np}(x)}{D_B},\ \ at\ y=0 \tag{5a}$$
$$u\to 0,\ T\to T_\infty,\ N\to N_\infty,\ \text{as}\ y\to\infty \tag{5b}$$

Here u and v denote the stream mechanism in the x and y information respectively, ν a kinematic viscosity, $\alpha=\dfrac{k}{\rho c_p}$ a thermal diffusivity, k a fluid density, ρ a thermal conductivity, c_p a specific heat, T a fluid temperature, T_∞ a ambient temperature, N a fluid concentration, C_∞ a ambient concentration, $\alpha=k/\rho c_p$ a thermal diffusivity, k a thermal conductivity, c_p a specific heat, $q_r=\dfrac{16\sigma^* T_\infty^3}{3k^*}\dfrac{\partial T}{\partial Y}$ a radiative heat flux, k^* a mean absorption coefficient, σ^* a Stefan-Boltzmann constant, $(\rho c)_p$ a consequence heat capacity of nanoparticles, $(\rho c)_f$ heat capacity of the base fluid. N is nanoparticle volume, D a mass diffusion $U_w(x)=\mathrm{U}_0\exp(x/l)$ is a stretched stream of sheet, U_0 a reference stream, l a reference length, $q_w(x)=q_{w0}\,\mathrm{T}_0\sqrt{U_0/2vl}\exp(x/l)$ the variable heat flux, $q_{np}(x)=q_{np0}C_0\sqrt{U_0/2vl}\exp(x/l)$ a variable surface nanoparticle flux, U_0, T_0, q_{w0}, q_{np0}, N_0, are the reference stream, temperature and heat flux, surface nanoparticle flux, nanoparticle capacityfraction respectively, $V(x)=V_0\exp(x/l)$ a special type of stream at the wall is considered (Bhattacharyya [30]) where V_0 is a constant. Here $V(x)>0$ is the stream of suction and $V(x)<0$ is the stream of injection.

Introducing similarity transformations as follows:

$$\eta = y\left(\frac{U_0}{2\nu x}\right)^{1/2}\exp\left(\frac{x}{l}\right),\ \psi = \left(2\nu U_0 x\right)^{1/2} f(\eta)\exp\left(\frac{x}{l}\right),$$
$$u = U_0 f'(\eta)\exp\left(\frac{x}{l}\right),\ v = -\sqrt{\frac{\nu U_0}{2l}}\exp\left(\frac{x}{l}\right)\left[f(\eta)-\eta f'(\eta)\right],$$
$$T = T_\infty + \frac{q_{w0}}{\alpha}T_0\exp\left(\frac{x}{l}\right)\theta(\eta), C = C_\infty + \frac{q_{np0}}{\alpha}C_0\exp\left(\frac{x}{l}\right)\phi(\eta) \quad (6)$$

If the dimensional stream function $\psi(x,y)$ then $u = \frac{\partial\psi}{\partial y}$ and $u = -\frac{\partial\psi}{\partial x}$.

The continuity equation is automatically satisfied and using similarity transformation, the system of Eqs. (2), (3) and (4) becomes:

$$f''' + ff'' - 2f'^2 - Ha^2 f' = 0 \quad (7)$$
$$\left(1+\frac{4}{3}R\right)\theta'' + \Pr\left(f\theta' + f'\theta + N_b\theta'\phi' + N_t\theta'^2\right) + \Pr Ec\left(f''\right)^2 = 0 \quad (8)$$
$$\phi'' + Le(f\phi' - f'\phi) + \frac{N_t}{N_b}\theta'' = 0 \quad (9)$$

Here primes mean differentiation with respect to η, $Ha = \frac{\sigma B_0^2(x)l}{\rho U_w(x)}$ is a Hartmann statistics, $\Pr = \frac{\nu}{\alpha}$ is a Prandtl statistics, $R = \frac{4\sigma^* T_\infty^3}{kk^*}$ is a emission constraint and $Le = \frac{\nu}{D_B}$ is a Lewis statistics, $N_b = \frac{(\rho c)_p q_{np0}}{(\rho c)_f \nu}N_0$ is a Brownian motion constraint, $Ec = \frac{U_0^2}{T_0\rho c_p}$ is a Eckert statistics, and $N_t = \frac{D_T}{T_\infty}\frac{(\rho c)_p q_{w0}}{(\rho c)_f \alpha\nu}T_0$ is a thermophoresis constraint, respectively.

The transformed frontier conditions (5a) and (5b) are given by

$$f(0) = S,\ f'(0) = -1,\ \theta(0) = -1,\ \phi(0) = -1$$
$$f'(\infty) = 0,\ \theta(\infty) = 0,\ \phi(\infty) = 0 \quad (10)$$

Where $S = \frac{-v_0}{\sqrt{\nu c/2l}}$ is suction/injection constraint. Here the constraint is positive $S>0$ ($v_0<0$) for mass suction and negative $S<0$ ($v_0>0$) for mass injection.

The substantial quantities of concern are the confined skin friction coefficient, the wall heat transport coefficient (or the confined Nusselt statistics) and the wall deposition flux (or the confined Stanton statistics) which are defined as respectively where the skin friction C_f, the heat transport $q_w(x)$ and the mass transport Sh_x from the wall are given by

$$\sqrt{2C_f \operatorname{Re}_x} = f''(0),\ C_f = \frac{u}{U_w\exp(x/l)}\left(\frac{du}{dy}\right)_{y=0}, \quad (11)$$

From the temperature field, we can study the rate of heat transport which is given by

$$\frac{Nu_x}{\sqrt{\operatorname{Re}_x}} = -\sqrt{\frac{x}{2l}}\left(1+\frac{4}{3}R\right)\theta'(0), Nu_x = -\frac{x}{(T_w - T_\infty)}\left(\frac{\partial T}{\partial y}\right)_{y=0} \quad (12)$$

From the concentration field, we can study the rate of mass transport which is given by

$$\frac{Sh_x}{\sqrt{\operatorname{Re}_x}} = -\sqrt{\frac{x}{2l}}\phi'(0),\ Sh_x = -\frac{x}{(C_w - C_\infty)}\left(\frac{\partial C}{\partial y}\right)_{y=0} \quad (13)$$

where $\operatorname{Re}_x = U_0 x/\nu$ the confined Reynolds statistics.

3. Method of solution:

The structure of ordinary differential equations (7) – (9) subject to the frontier conditions (10) are solved numerically using Runge–Kutta fourth-order integration with shooting technique. A step size of $\Delta\eta = 0.01$ was selected to be satisfactory for a convergence criterion of 10^{-6} in all cases. The grades are obtainable graphically in Figs. (1) –(7) and conclusions are drawn for stream field and other physical quantities of interest that have noteworthy consequences.

4. Results and discussion:

Eqs. (7)–(9) with frontier conditions (10) are numerically solved using the Runge–Kutta fourth-order integration with shooting method, and numerical values are presented in Figs. (1)–(9). (7). Throughout the computations, the leading constraints are kept constant at Ha=1.0, S = 3.0, Le = 1.3, R = 0.1, Pr = 0.71, Ec=0.1, Nt = 0.8, and Nb = 0.5. On the stream, temperature, and particles of nano sized capacity friction profiles, the consequence of the involved constraints suction constraint Hartmann statistics, Eckert statistics Ec, Lewis statistics Le, emission constraint R, thermophoresis statistics Nt, and Brownian motion constraint Nb. Figures 1(a)-(b) show the stream, temperature, and nanoparticle capacityfriction profiles for various suction constraint values.

The stream profiles rise as the suction constraint is increased, as shown in Fig. 1(a). Figure 1(b) further shows that as the suction constraint is increased, the temperature drops. In Figs 2(a)-(b), the consequence of the Hartmann statistics (i.e. magnetic field constraint Ha) on the stream, temperature, and nano-particle capacity friction profiles is shown. The stream profiles rise with higher values of Hartmann statistics, as shown in Fig. 2(a). The Lorentz force increases when the magnetic field is increased physically. The fluid's stream is raised as more resistance is applied to the fluid's motion. The temperature drops as the Hartmann statistics rises, as shown in Fig. 2(b).

The work of the dissipative constraint, Eckert statistics Ec, on the stream and temperature profiles is shown in Fig. 3(a)-(b). The stream and temperature profiles of the stream are observed to grow as the dissipation constraint Ec is increased. In general, increasing viscosity increases heat conductivity, which leads to increased stream profiles. The consequences of the thermophoresis constraint Nt on temperature and nano-particle capacity fraction are shown in Fig. 4(a)-(b). The temperature (Fig. 4(a)) and nano-particle capacity fraction (Fig. 4(b)) profiles both increase as the thermophoresis constraint is increased. The ratio of nanoparticle diffusion to thermal diffusion in the nanofluid is the thermophoresis constraint Nt.
The temperature differential between the sheet and the fluid grows as Nt increases, and the thermal frontier layer expands in this situation. Thermophoresis force increases as Nt increases, allowing the nano-particle to migrate from hot to cold regions. The capacity fraction of nano-particles increases as a result of this migration. The consequence of the emission constraint R on temperature and nano-particle capacity fraction profiles is shown in Fig. 5(a)-(b). It's worth noting that higher R values improve the temperature profile. This is owing to the fact that when R increases, the mean absorption coefficient decreases. The nano-particle capacity fraction profile increases as R increases, as shown in Fig. 5(b).

Finally, Figs. (6) and (7) show how the Lewis statistics *Le* and the Brownian motion constraint *Nb* affect the nano-particle capacity fraction profiles. The distribution of nano-particle capacity fraction diminishes as the Lewis statistics increases, as shown in Fig. (6). This is likely due to the fact that when Le increases, the Brownian diffusion coefficient *Nb* decreases, limiting nano-particles' ability to penetrate further into the fluid. As a result, at a larger Lewis statistics Le, the capacity fraction of nano-particles is thinner. Furthermore, as the Brownian motion constraint *Nb* is increased, the nano-particle capacity fraction profile decreases. This could cause the thermal frontier layer to thicken. Physically, an increase in Brownian motion generates an increase in nano-particle diffusion, which lowers the concentration inside the frontier layer.

Table 1& Table 2 illustrate mathematical information on the consequences of assorted constraints on the friction factor term, Nusselt statistics, and Sherwood statistics. Table 1 indicates that raising the values of the emission constraint *R* and the Eckert statistics Ec lowers the skin friction coefficient, whereas increasing the values of *R* and *Ec* raises the Nusselt statistics. Table 2 presences that when the significance of *Ha* increases, the confined Nusselt statistics and Sherwood statistics drop, whereas the opposite is true for higher values *S*.

Table 1: **S**tatistical values of friction factor term and confined Nusselt statistics for different values of *Ec* and *R* when *Ha*=1.0, *Nt*=0.8, *Nb*=0.5, *Pr*=0.71, *R*=0.1, *Ec*=0.1 and *Le* = 1.3.

Constraints(fixed values)	Constraints	$f''(0)$	$\mathrm{Re}_x^{-1/2} Nu_x$
Nt=0.8, *Nb* = 0.5, *S*=3.0, *Pr*=0.71, *R*=0.1, *Le*=1.3	*R*=0.10	1.120557	0.460557
	0.15	1.116654	0.466654
	0.30	1.097774	0.467774
	Ec=0.0	1.165307	0.459307
	0.1	1.120557	0.460557
	0.2	1.108726	0.468726

Table 2: Numerical values of confined Nusselt statistics and confined Sherwood statistics for different values of *Ha* and *S* when *Ha*=1.0, *Nt*=0.8, *Nb*=0.5, *Pr*=0.71, *R*=0.1, *Ec*=0.1 and *Le* = 1.3.

Constraints(fixed values)	Constraints	$\mathrm{Re}_x^{-1/2} Nu_x$	$\mathrm{Re}_x^{-1/2} Sh_x$
Nt=0.8, *Nb* = 0.5, *S*=3.0, *Pr*=0.71, *R*=0.1, *Le*=1.3	*Ha*=1.0	0.451145	0.294788
	1.5	0.438589	0.287824
	3.0	0.403746	0.267842
	S=0.5	0.415307	0.251433
	0.6	0.423403	0.262577
	0.8	0.440726	0.278440

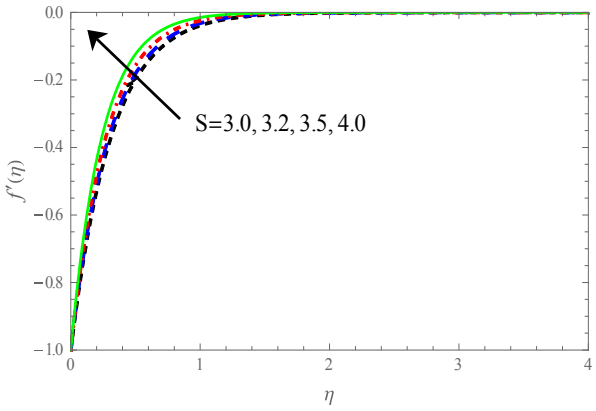

Fig 1(a). Consequence of s on $f'(\eta)$

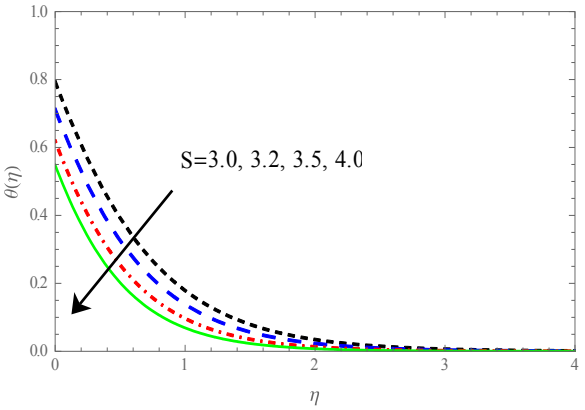

Fig 1(b). Consequence of s on $\theta(\eta)$

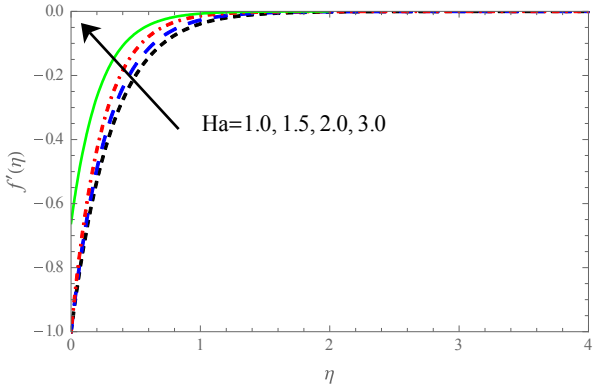

Fig 2(a). Consequence of Ha on $f'(\eta)$

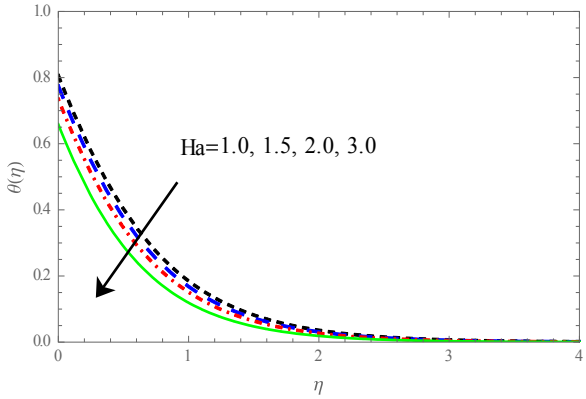

Fig 2(b). Consequence of Ha on $\theta(\eta)$

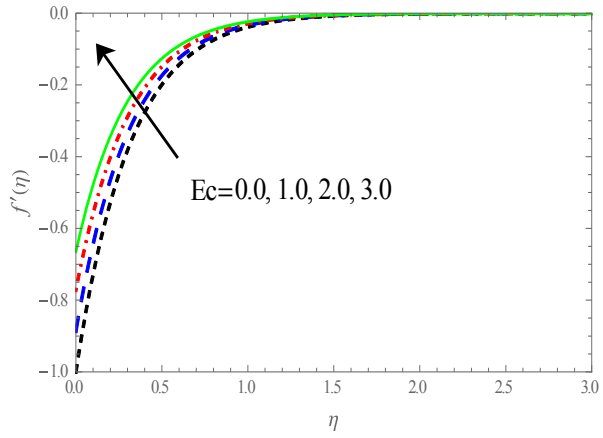

Fig 3(a). Consequence of Ec on $f'(\eta)$

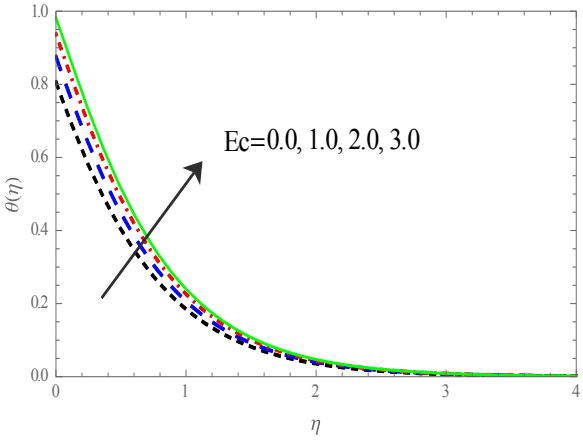

Fig 3(b). Consequence of Ec on $\theta(\eta)$

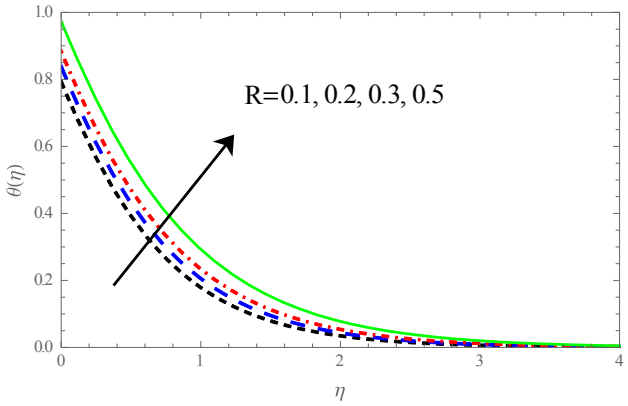

Fig 4(a). Consequence of R on $\theta(\eta)$

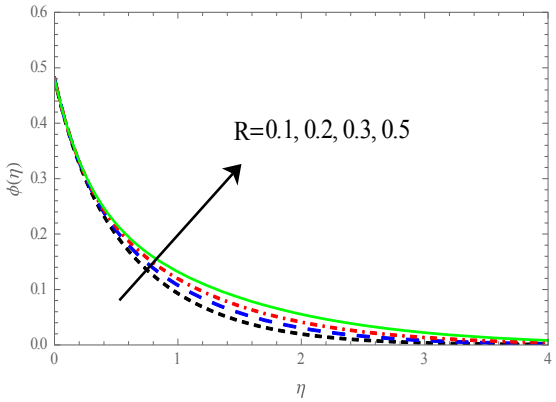

Fig 4(b). Consequence of R on $\phi(\eta)$

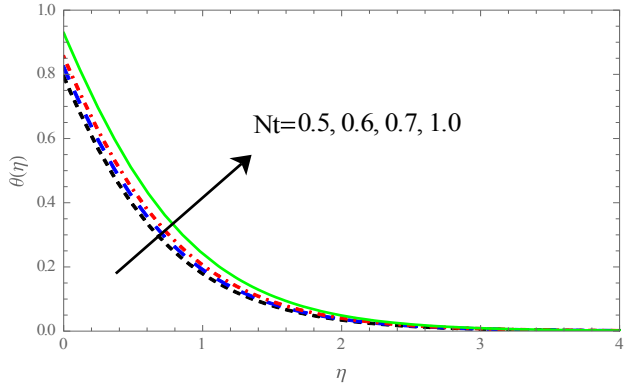

Fig 5(a). Consequence of Ec on $\theta(\eta)$

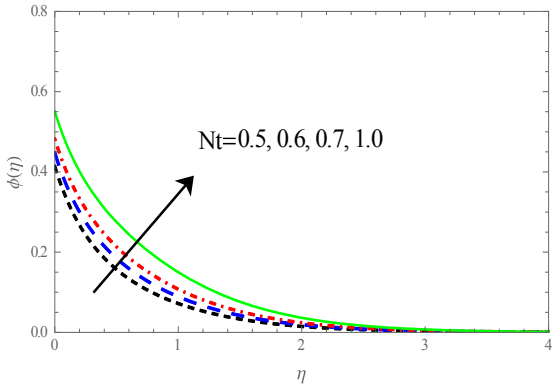

Fig 5(b). Consequence of Ec on $\phi(\eta)$

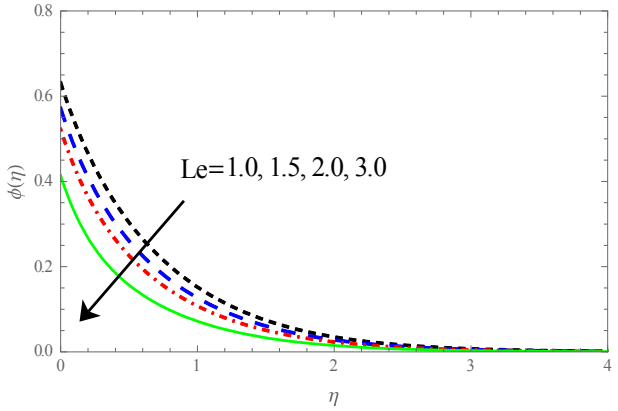

Fig 6. Consequence of Le on $\phi(\eta)$

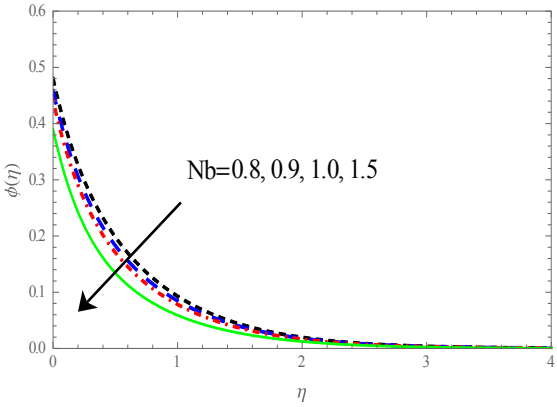

Fig 7. Consequence of Nb on $\phi(\eta)$

5. Conclusion:

The importance of thermal emission and Magneto-hydro-dynamics (MHD) in the stream of a viscous dissipating nanofluid, as well as heat transport analysis using an exponentially starching sheet with warm and mass flux conditions with viscous dissipation, are presented in this work. Using suitable transformations, the leading partial differential equations were converted into a set of nonlinear coupled ordinary differential equations, and the resultant well-posed frontier value problem was numerically solved using the Runge–Kutta fourth order based shooting method. The implications

of relevant constraints on the fields of stream, temperature, and nano-particle capacity friction, skin friction, heat, and mass transport coefficients are addressed and illustrated in graphs and tables. The following are the key conclusions drawn from this research:

(i) Stream profile and frontier layer thickness increase via suction constraint S, Hartmann statistics *Ha* and Eckert statistics *Ec*.
(ii) Temperature profile and thermal frontier layer thickness yields a decrease via larger suction constraint *s*, Hartmann statistics *Ha*, but they reduces by increasing emission parameter *R* and Eckert statistics *Ec*.
(iii) The nano-particle capacity fraction increases as the value of emission constraint *R* and thermophoresis constraint *Nt* increases.
(iv) Skin fraction coefficient decrease as the value of constraints *R* and *Ec*.
(v) Confined Nusselt statistics is increasing function of S, *R* and *Ec*.
(vi) Confined Sherwood statistics is increasing function of S.

References:

[1] Crane, L .J., Flow past a stretching plate. Zeitschrift für angewandte Mathematik und Physik *ZAMP*, Vol. 21, No. 4, 1970, pp. 645–647.

[2] Dutta, B. K, Roy P, Gupta, A.S. Temperature field in flow over a stretching sheet with uniform heat flux. *Int Commun Heat Mass Transform* , Vol. 12, No. 1, 1985, pp. 89–94.

[3] Char, M.I. Heat transform of a continuous, stretching surface with suction or blowing. *J Math Anal Appl.,* Vol. 135, No. 2, 1988, pp. 568–80.

[4] Gupta ,P.S., and Gupta, A.S., Heat and mass transform on a stretching sheet with suction or blowing. *Can J Chem Eng,* Vol. 55, No. 6, 1977, pp. 744–746.

[5] Nadeem S, Haq R.U., and Khan Z .H., Heat transform analysis of water-based nanofluid over an exponentially stretching sheet. *Alexandria Eng. J.,* Vol. 53, No. 1, 2014, pp. 219–224.

[6] Bhattacharyya, K., Boundary layer flow and heat transform over an exponentially shrinking sheet, *Chin. Phys. Lett.,* Vol. 28, No. 7, 2011, pp. 1-10.

[7] Mukhopadhya S., Slip effects on MHD Boundary layer flow over an exponentially stretching sheet with suction/blowing and thermal radiation. *Ain Shams Eng J.,* Vol. 4, No. 3, 2013, pp. 485–491.

[8]. Sajid, M., Hayat, T. Influence of thermal radiation on the boundary layer flow due to an exponentially stretching sheet, *Int. Commun. Heat Mass Transf.* vol. 35, 2008, pp. 347–356.

[9] Zhang, Y. Zhang, M, Bai Y., Unsteady flow and heat transform of power-law nanofluid thin film over a stretching sheet with variable magnetic field and power-law flow slip effects, *J. Taiwan Inst Chem Eng*., Vol. 70, 2017, pp. 104–110.

[10] Majeed A, Zeeshan A, Ellahi R, Unsteady ferromagnetic liquid flow and heat transform analysis over a stretching sheet with the effect of dipole and prescribed heat flux, *J Mol Liq*, Vol. 223, 2016, pp. 528–533.

[11] Pal D, Saha P, Influence of nonlinear thermal radiation and variable viscosity on hydromagnetic heat and mass transform in a thin liquid film over an unsteady stretching surface. *Int J Mech Sci,* Vol. 119, 2016, pp. 208–216.

[12] Weidman P, Turner M R, Stagnation-point flow with stretching surfaces: a unified formulation and new results. *Eur J Mech B Fluids,* Vol. 61, 2017, pp. 144–153.

[13] S. Mukhopadhyay, I.C. Moindal, T. Hayat MHD boundary layer flow of Casson fluid passing through an exponentially stretching permeable surface with thermal radiation, *Chin. Phys*. B, Vol. 23, 2014, pp. 104701-12.

[14] T. Hayat, M. Imtiaz, A, Alsaedi, Impact of magnetohydrodynamics in bidirectional flow of nanofluid subject to second order slip flow and

homogeneous–heterogeneous reactions, *J. Magn. Magn. Mater*., Vol. 395, 2015, pp. 294–302.

[15] Y. Lin, L. Zheng, X. Zhang, L. Ma, G. Chen, MHD pseudo-plastic nanofluid unsteady flow and heat transform in a finite thin film over stretching surface with internal heat generation, *Int. J. Heat Mass Transf.,* Vol. 84, 2015, pp. 903–911.

[16] M. Sheikholeslami, D.D. Ganji, M.Y. Javed, R. Ellahi. Effects of thermal radiation on magnetohydrodynamics nanofluid flow and heat transform by means of two phase model, *J. Magn. Magn. Mater.,* Vol. 374, 2015, pp. 36–43.

[17] U. Farooq, Y.L. Zhao, T. Hayat, A. Alsaedi, S.J. Liao. Application of the HAM-based Mathematica package BVPh 2.0 on MHD Falkner–Skan flow of nanofluid, *Comput. Fluids,* Vol. 11, 2015, pp. 69–75.

[18] S.A. Shehzad, Z. Abdullah, A. Alsaedi, F.M. Abbaasi, T. Hayat. Thermally radiative three-dimensional flow of Jeffrey nanofluid with internal heat generation and magnetic field, *J. Magn. Magn. Mater*., Vol. 397, 2016, pp. 108–114.

[19] A. Moradi, H. Ahmadikia, T. Hayat, A. Alsaedi, On mixed convection radiation interaction about an inclined plate through a permeable medium, *Int. J. Thermal Sci.* Vol. 64, 2013, pp. 129–136.

[20] M. Sheikholeslami, D.D. Ganji, M.Y. Javed, R. Ellahi, Effect of thermal radiation on magnetohydrodynamics nanofluid flow and heat transform by means of two phase model, *J. Mag. Magnetic Materials,* Vol. 374, 2015, pp. 36–43.

[21] T. Hayat, S. Hussain, A. Shehzad, A. Alsaedi, Flow of Oldroyd-B fluid with nanoparticles and thermal radiation, *Appl. Math. Mech.* Vol. 36, 2015, pp. 69-80.

[22] M. Ashraf, T. Hayat, S. Shehzad, A. Alsaedi, Mixed convection radiative flow of three dimensional Maxwell fluid over an inclined stretching sheet in occurrence of thermophoresis and convective condition, *AIP Adv.* Vol. 5, 2015, pp. 027134 - 44.

[23] Hayat T., N. Gull, M. Farooq, B. Ahmad, Thermal radiation effects in MHD flow of Powell-Eyring nanofluid induced by a stretching cylinder, *J. Aerospace Eng., ASCE*. Vol. 29, No. 1, 2015, pp. 1943-1955.

[24] Bidin B and Nazar R, Numerical Solution of the Boundary layer flow over an Exponentially Stretching Sheet with Thermal Radiation, *Eur. J. Sci. Res.* Vol. 33, No. 4, 2009, pp. 710–717.

[25] Hady F.M, Ibrahim F.S, Abdel-Gaied S.M, Eid M.R, radiation effects on viscous flow of a nanofluid and heat transform over a nonlinearly stretching sheet, *Nano Scale Res Lett*, Vol. 7, 2012, pp. 299-312.

[26] Hayat T., M. Waqas, S.A. Shehzad, A. Alsaedi, Effects of Joule heating and thermophoresis on stretching flow with convective boundary layer connditions, *Scientia Iranica,* Vol. 21, 2014, pp. 682–692.

[27] M. Mustafa, J. Khan, T. Hayat, A. Alsaedi,. Sakiadis flow of maxwell fluid considering magnetic field and convective boundary conditions, *AIP Adv.,* Vol. 5, 2015, pp. 27106 - 11.

[28] Hayat T., M. Waqas, S. Shehzad, A. Alsaedi, Mixed convection radiative stream of Maxwell fluid near a stagnation point with convective condition, *J. Mech.* Vol. 29, 2013, pp. 403–409.

[29] Hayat T., S. Qayyum, A. Alsaedi, A. Shafiq, Inclined magnetic field and heat source/sink aspects in flow of nanofluid with nonlinear thermal emission, *Int. J. Heat Mass Transport* , Vol. 103, 2016, pp. 99–107.

[30] Khan, M. Khan, W.A., Alshomrani, A.S. Non-linear radiative flow of three dimensional Burgers nanofluid with new mass flux effects, *Int. J. Heat Mass Transform*, Vol. 101, 2016, pp. 570–576.

AUTHORS' CONTRIBUTIONS: All authors have contributed equally to this.